Journal of
Materials Chemistry A

Materials for energy and sustainability

Accepted Manuscript

This article can be cited before page numbers have been issued, to do this please use: A. E. King, J. J. Bailey, J. Le, A. H. Turner, R. N. Purusottam, E. Dahlqvist, A. Martinelli, M. Swadzba-Kwasny and J. D. Holbrey, *J. Mater. Chem. A*, 2026, DOI: 10.1039/D6TA02268E.

ROYAL SOCIETY OF CHEMISTRY

rsc.li/materials-a

View Article Online
DOI: 10.1039/D6TA02268E

Journal Name

ARTICLE TYPE

Cite this: DOI: 00.0000/xxxxxxxxxx

Modulating transport properties in *N*-alkyl-4-cyanopyridinium ionic liquids through formation of liquid charge transfer complexes†

Aloisia E. King,[a] Josh J. Bailey,[a] Jiabo Le,[a,b] Adam H. Turner,[a,c] Rudra N. Purusottam,[a] Eva Dahlqvist,[d] Anna Martinelli,[d] Małgorzata Swadźba-Kwaśny,[a] and John D. Holbrey[a*]

Received Date
Accepted Date

DOI: 00.0000/xxxxxxxxxx

The impact of liquid charge-transfer complex formation between nitrile-functionalised *N*-alkyl-4-cyanopyridinium bis(trifluoromethylsulfonyl)imide ionic liquids ([C_n^{4}CNPy][NTf_2], n = 1–4) and 1-methylnaphthalene on conductivity and viscosity of the liquids has been investigated. These ionic liquids exhibit higher viscosities and lower conductivities than N-butylpyridinium bis(trifluoromethylsulfonyl)imide, confirming the role of the nitrile group in strengthening ion association as previously identified by Hardacre *et al.* (*Phys. Chem. Chem. Phys.*, 2010, **12**, 1842). Strikingly, [C_2^{4}CNPy][NTf_2] displays anomalous viscosity-conductivity behaviour, deviating from homologous trends. Formation of charge transfer complex liquids with one equivalent of 1-methylnaphthalene suppresses these anomalies, producing convergent transport profiles and revealing how π–π interactions reshape nanoscale structure and dynamics. These findings provide new insight into tailoring ionic liquid properties through molecular design and controlled charge-transfer interactions.

Introduction

Ionic liquids (ILs), by definition, are fluids that predominantly comprise of ions and so are intrinsically electrically conductive through ion transport mechanisms. This characteristic is exploited in their use as electrolytes,[1] although their inherent ionic conductivity is relatively low compared to conventional electrolyte solutions. One strategy to increase conductivity is through the addition of a diluent. While this reduces the effective ionic strength, reduction in viscosity[2] leads to an increase conductivity,[3] albeit at the expense of introducing a potentially volatile and/or redox-active component. The extent to which conductivity can be enhanced through the reduction in viscosity is determined by the degree of competition between favourable dissociative or unfavourable associative interactions between the ions and diluent molecules.[4] For example, it has been shown that the viscosity of [C_4mim][NTf_2] is reduced by *ca.* 60-80%, from around *ca.* 50 cPs to 10-20 cPs (at 298 K), on addition of 1 molar equivalent of acetonitrile, methanol, dichloromethane, water, or 1-butanol.[5]

We have re-examined a series of ionic liquids with *N*-alkyl-4-cyanopyridinium cations[6–8] originally explored as potential media for aromatic extraction from hydrocarbons (dearomatisation and desulfurisation of diesel fuels)[9] and most recently for selective gas absorption.[10] These ILs form highly coloured charge-transfer (CT) complexes in the presence of electron-rich aromatic guest molecules, such as 1-methylnaphthalene (1-MN) as shown in Fig. 1. This association leads to the formation of columnar stacks of alternating cations and aromatic molecules in 1:1 co-crystals of [C_1^{4}CNPy][NTf_2], and [C_2^{4}CNPy][NTf_2] with 1-MN, and to brightly coloured liquids with evidence for extended CT complex stacking beyond first shell correlation through neutron scattering studies and molecular dynamics simulations.[8] Interestingly, the isomeric *N*-methyl-3-cyanopyridinium and *N*-methyl-2-cyanopyridinium bis(trifluoromethanesulfonyl)imide crystallise as pure salts from their corresponding coloured liquid CT complexes.

The conductivities of these *N*-alkyl-4-cyanopyridinium ILs and their CT complex mixtures with polyaromatic donors has not previously been reported, nor has the effect of 1-MN addition on the viscosities of the resultant IL:1-MN mixtures. Here we explore

[a] The QUILL Research Centre, School of Chemistry and Chemical Engineering, Queen's University Belfast, David Keir Building, Stranmillis Road, Belfast BT9 5AG, UK. E-mail: j.holbrey@qub.ac.uk
[b] Current address: Zhejiang Key Laboratory of Advanced Fuel Cells and Electrolyzes Technology, Ningbo Institute of Materials Technology and Engineering, Chinese Academy of Sciences, Ningbo 315201, China
[c] Current address: Department of Chemistry, Ateneo de Manila University, Quezon City 1108, Philippines
[d] Department of Chemistry and Chemical Engineering, Chalmers University of Technology, Gothenburg 41296, Sweden
† Electronic Supplementary Information (ESI) available: Synthetic and analytical data; viscosity, conductivity, and DOSY NMR data. See DOI: 00.0000/00000000.

View Article Online
DOI: 10.1039/D6TA02268E

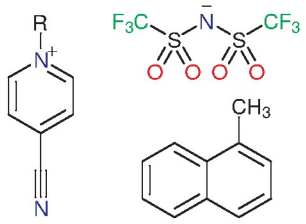

Fig. 1 Structures of the ionic liquid cation, $[C_n{}^4CNPy]^+$ (n = 1–4), anion, $[NTf_2]^-$, and 1-methylnaphthalene (1-MN).

the effect of CT complex formation between the electron-rich aromatic donor and $[C_n{}^4CNPy]^+$ cations on the viscosity and conductivity of the ILs, $[C_n{}^4CNPy][NTf_2]$ (n = 1–4) and their 1:1 mixtures with 1-MN.

Redox active mixtures of ionic liquids containing two cations, one with an appended carbazole group as an electron donor and one based on viologen cations as electron acceptors have been shown to form a CT complex[11] in which both viscosity and conductivity were reduced upon CT formation. Potential applications in electrochemical reactions and devices, supercapacitors, redox flow batteries, electrochromic devices, and electron mediators for photochemical catalysis have been proposed.[12]

In particular, we were interested to examine what the impact of CT complex formation would be on the thermophysical and electrochemical behaviour of the systems and determine whether typical diluent effects, *e.g.*, reduction in viscosity and commensurate increase in conductivity, would be observed, or whether the CT complex association of cations and aromatic donors might lead to long length-scale aggregation and different behaviour. One possible envisaged scenario was that columnar-aromatic aggregation with sufficiently long-range order, resembling that previously identified in the crystal structures for the n = 1 and n = 2 salts, may be present. It was hypothesised that this structure might provide a pathway for electron transport along the CT stacks, thus enhancing overall conductivity, in a similar way that has been seen in the induction of 1-dimensional conduction in columnar discotic liquid crystals.[13]

Experimental

Materials and methods

All chemicals were used as received unless noted. Pyridine, dimethyl sulfate, and other dialkyl sulfates were sourced from Merck and TCI Chemicals; $Li[NTf_2]$ from 3M; 4-cyanopyridine from Fluorochem; and bromobutane from Acros Organics. All chemicals were >96% purity, except dipropyl sulfate (>90%), and were used as received unless otherwise stated.

Synthesis

N-alkyl-4-cyanopyridinium alkylsulfate salts were prepared by alkylation of 4-cyanopyridine with dialkyl sulfates. $[C_1{}^4CNPy][CH_3SO_4]$ and $[C_2{}^4CNPy][C_2H_5SO_4]$ were synthesised following literature methods,[6] while $[C_3{}^4CNPy][C_3H_7SO_4]$ and $[C_4{}^4CNPy][C_4H_9SO_4]$ were obtained *via* solvent-free alkylation at 100 °C as described in the ESI. This approach avoids long reaction times or pressurised conditions required for the alkylation with bromobutane.[6,14] The *N*-alkyl-4-cyanopyridinium bis(trifluoromethanesulfonyl)imide ILs were then prepared by anion exchange with $Li[NTf_2]$ in water. Reference ILs, 1-ethyl-3-methylimidazolium bis(trifluoromethanesulfonyl)imide ($[C_2mim][NTf_2]$)and *N*-butylpyridinium bis(trifluoromethanesulfonyl)imide ($[C_4Py][NTf_2]$) were synthesised following established literature procedures after N-alkylation with bromoethane and bromobutane respectively.[15,16] Energy dispersive X-ray fluorescence (EDXRF, Rigaku NEX QC+ QuantEZ) was used to determine that the residual bromide content was <55 ppm in both cases. All the ILs were characterised by ^1H and ^{13}C NMR spectroscopy, Raman spectroscopy, MS and CHNS elemental analysis, TGA, DSC, as well as viscosity and conductivity measurements. $[C_3{}^4CNPy][NTf_2]$ is newly reported and fully characterised in the ESI; other ILs matched literature data.[6,14]

Viscosity Measurements

Viscosities were measured using an Anton Paar MCR302e Rheometer (±0.2 °C) and SVM 3001 Viscometer (±0.005 K, accuracy ~0.1%). Measurements were performed at ambient pressure for neat ILs and mixtures with 1-MN or acetonitrile. Water contents, determined by Karl Fischer titration (Metrohm 899 Coulometer), were <228 ppm for all neat ionic liquids (average 160 ppm). IL:1-MN samples were prepared by combining appropriate masses of the ILs with 1-MN (111 ppm water) between *ca.* 2.8–3.1:1 mass ratios. Literature indicates that water contents <200 ppm are below the threshold for significant influence on viscosity,[17] particularly for $[NTf_2]^-$-based ILs.[18] Full datasets and conditions are provided in the ESI.

Conductivity Measurements

Conductivity was determined by electrochemical impedance spectroscopy (EIS) using a custom glass cell with a 6 mm diameter graphite working electrode and stainless-steel mesh counter electrode, immersed in a temperature-controlled oil bath (Heidolph MR Hei-Tec). A 14 mV root-mean-squared amplitude voltage perturbation was applied over a frequency range of 1 kHz to 1 MHz. The cell constant was calibrated using $[C_4Py][NTf_2]$, selected for its structural similarity and well-documented properties.[19–21] The conductivity of $[C_4Py][NTf_2]$ (180 ppm water) at 22.5 °C was 2.88 mS cm^{-1} (Hach Sension+ EC71 conductivity meter, calibrated against aqueous KCl standards of conductivity 147 μS cm^{-1}, 1413 μS cm^{-1}, and 12.88 mS cm^{-1}) consistent with mean values from data[20,22] in the NIST ILThermo database.[23] This value was used to determine the cell constant for EIS.

Measurements for neat ILs and IL:1-MN mixtures were performed in triplicate, with final values obtained from the best-fit line of the triplicate data. Impedance data were analysed in RelaxIS 3 (RHD Instruments) using an equivalent circuit

View Article Online
DOI: 10.1039/D6TA02268E

model; conductivity was calculated from combined resistance values (R_1 + R_2) and the calibrated cell constant. Full details, including Arrhenius plots and model fits, are provided in the ESI.

DOSY NMR

The diffusivities of the cation, anion and 1-MN in the neat ILs and IL:1-MN CT liquids (n = 2–4) were determined at 333 K using ^{1}H and ^{19}F DOSY NMR on a Bruker AV600 NMR spectrometer. Spectra were collected using the 1D LED using bipolar gradients(ledbpgp2s) 2D sequence for diffusion measurement.[24] Analysis of the DOSY spectral signals was performed with Bruker TopSpin 5.0.0 and Dynamics Center 2.8.9 by curve fitting using the Stejskal-Tanner diffusion fit function (equ. (1)).[25]

$$f(g) = I_0 \times exp[-D \cdot (\gamma^2 \delta^2 g^2) \cdot (\Delta - \delta/3)] \quad (1)$$

^{1}H diffusion coefficients were comparable for all ^{1}H signals in each individual cation or and 1-MN in IL:1-MN mixtures. Mean values of D_{cation} and D_{1-MN} are presented as averages across all the proton signals of either the cation (N-alkyl and aromatic) or 1-MN (methyl and aromatic) respectively. Values for the individual signals are tabulated in ESI. The ^{19}F NMR spectrum exhibited one peak at *ca.* –79 ppm, assigned to the $[NTf_2]^-$ anion in each case.

Raman Spectroscopy

Raman spectra were collected for all samples at room temperature, using two lasers, one with a wavelength of 532 nm and the other with a wavelength of 785 nm. Using the 785 nm laser, most spectra appeared clean. In contrast, excitation at 532 nm produced a strong fluorescence background for several samples, particularly $[C_3{}^4CNPy][NTf_2]$ and $[C_4{}^4CNPy][NTf_2]$. However, the 532 nm laser did allow clear resolution of the wavenumber region above 3000 cm^{-1}, where the ring C–H stretching modes are observed. The Raman spectra provide information on the conformational state of the $[NTf_2]^-$ anion (below 500 cm^{-1}), on the strength of interaction between the $[NTf_2]^-$ anion and its surrounding environment (720–760 cm^{-1}) as well as on the C≡N bond length through its stretching mode (2200–2300 cm^{-1}).

Results and Discussion

The conductivity and viscosity of the four $[C_n{}^4CNPy][NTf_2]$ ILs and their 1:1 IL:1-MN CT complex liquids were investigated. The optimal molar ratio of IL:1-NM for CT complex formation was determined through a Job plot analysis, using 0.1 M total concentration solutions of $[C_1{}^4CNPy][NTf_2]$+1-MN in acetonitrile, monitoring the solution absorbance band at 375 nm, as shown in Fig. 2. Equivalent Job plot profiles from $[C_1{}^4CNPy][NTf_2]$ and other polyaromatic donors (pyrene, anthracene, and dibenzothiophene) revealed similar optimal complex formation at the 1:1 ratio (shown in the ESI) suggesting that CT-association could also extend to many polyaromatic systems including graphitic surfaces, or doped carbon nanostructures.

The 1:1 ratio also matches the stoichiometry of the crystalline CT complexes previously isolated on cooling mixtures of 1-MN with $[C_1{}^4CNPy][NTf_2]$ and $[C_2{}^4CNPy][NTf_2]$.[8] It is worth noting that the limiting co-miscibilities of the $[C_n{}^4CNPy][NTf_2]$ ILs with 1-MN is not 1:1, but has been reported to increase from 1:1.2 for $[C_1{}^4CNPy][NTf_2]$, to 1:2.6 for $[C_2{}^4CNPy][NTf_2]$, to 1:4 for $[C_4{}^4CNPy][NTf_2]$, while $[C_6{}^4CNPy][NTf_2]$ is completely miscible with 1-MN. The co-miscibility limits of these ILs with 1-MN is significantly lower than that of $[C_4Py][NTf_2]$ or $[C_4mim][NTf_2]$ where ratios of 1:15 and 1:10.2 IL:1-MN have been reported.[8,26]

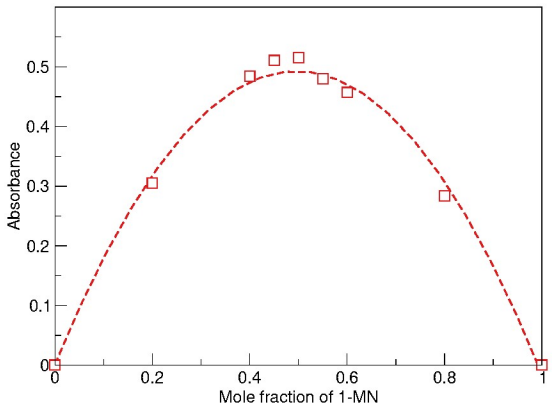

Fig. 2 Job's plot analysis showing maximum absorbance in the UV–vis spectrum at 375 nm from formation of the 1:1 CT complex between $[C_1{}^4CNPy][NTf_2]$ and 1-MN in MeCN with total concentration of IL and 1-MN of 0.1 M.

Viscosity and Conductivity profiles of neat $[C_n{}^4CNPy][NTf_2]$ ionic liquids

Viscosity and conductivity measurements for the four $[C_n{}^4CNPy][NTf_2]$ salts were measured over the temperature range 313-420 K (viscosity: 358-388 K; conductivity: 313-420 K). The viscosities of the four ILs (n = 1–4) are shown in Fig. 3. Most measurements were conducted above 358 K, the melting point of the 1:1 $[C_1{}^4CNPy][NTf_2]$:1-MN CT complex. Data for n = 2 and n = 4 are consistent with the literature[6,10,14] and are compared in the ESI, while data for n = 1 and n = 3 are reported here for the first time.

All four $[C_n{}^4CNPy][NTf_2]$ ILs are more viscous than analogous pyridinium and 4-methylpyridinium salts, reflecting the role of the electron-withdrawing nitrile substituent enhancing ion association. Viscosity decreases with shorter N-alkyl chains (butyl > propyl > methyl) as expected due to the reduction in 'drag' associated with the size of the N-alkyl substituent. $[C_2{}^4CNPy][NTf_2]$ deviates from this trend, however, exhibiting an anomalously elevated viscosity that is comparable to that of the butyl analogue, rather than intermediate between the values for the methyl and propyl-substituted ILs.

This anomaly does not appear to be due to impurities in the samples. The results were reproducible across replicate synthesised batches of $[C_2{}^4CNPy][NTf_2]$. Moreover, the melting point determined by DSC and viscosity are consistent with those previously reported from crystallographically characterised

View Article Online
DOI: 10.1039/D6TA02268E

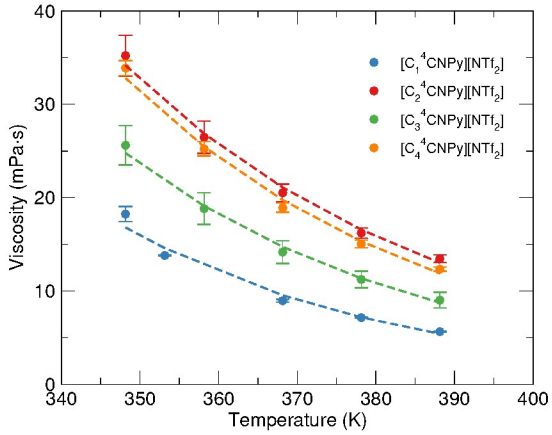

Fig. 3 Viscosities of neat $[C_n{}^4CNPy][NTf_2]$ (n = 1–4) ILs between 358-388 K, with lines showing fits of the data to the Vogel–Fulcher–Tammann equation.

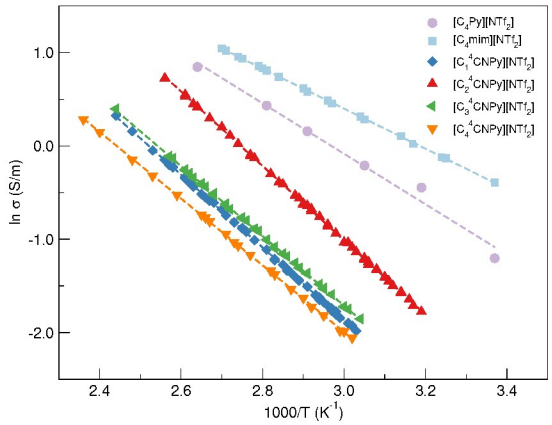

Fig. 4 (a) Arrhenius plots of conductivity (ln σ vs 1000/T, 313-420 K) for the neat ILs; $[C_1{}^4CNPy][NTf_2]$ (blue), $[C_2{}^4CNPy][NTf_2]$ (red), $[C_3{}^4CNPy][NTf_2]$ (green), and $[C_4{}^4CNPy][NTf_2]$ (orange), with dashed lines showing logarithmic fit of the data as a guide to the eye. Data for the reference ILs, $[C_4Py][NTf_2]$ and $[C_2mim][NTf_2]$, are shown for comparison.

$[C_2{}^4CNPy][NTf_2]$.[7] Furthermore, the presence of small molecule impurities (solvents, water, *etc.*) tend to reduce IL viscosity, as seen from the effects of adding acetonitrile to $[C_4{}^4CNPy][NTf_2]$ as described below. Instead, it likely reflects enhanced cation-cation association through nitrile interactions, as previously observed in solid-state[7] and liquid-phase[8] studies.

Conductivities derived from EIS (Fig. 4) reveal Arrhenius behaviour across the temperature range 320-420 K. All four ILs exhibit lower conductivities than non-nitrile analogues ($[C_4Py][NTf_2]$[20,22] and $[C_2mim][NTf_2]$[27,28]) consistent with their higher viscosities. Activation energies for conduction, determined from the slopes of the ln(conductivity) *vs* 1000/T plots in Fig. 4, are similar for all four $[C_n{}^4CNPy][NTf_2]$ ILs, and fall in the range 29.8 to 31.9 kJ mol^{-1}, which is typical for moderately viscous ILs (18–40 kJ mol^{-1}). By comparison, the activation energies of the less viscous and more conductive $[C_4Py][NTf_2]$ and $[C_2mim][NTf_2]$ were 22.3 kJ mol^{-1} (lit.[20,22] 27.0 kJ mol^{-1}) and 17.8 kJ mol^{-1} (lit.[27,28] 21.9 kJ mol^{-1}).

Importantly, the conductivities far exceed those of protic N-alkyl-4,5-dicyanoimidazolium ILs.[29] These are the only other nitrile-functionalised aromatic cation systems for which data exist; however, their protic nature may lead to more extensive hydrogen bonding between ions. The relative ranking of the conductivities of $[C_3{}^4CNPy][NTf_2]$ and $[C_4{}^4CNPy][NTf_2]$ are as expected, with $[C_3{}^4CNPy][NTf_2]$ having higher conductivity consistent with its lower viscosity compared to $[C_4{}^4CNPy][NTf_2]$. Interestingly, the conductivity of $[C_2{}^4CNPy][NTf_2]$ is higher than that of the corresponding ILs with propyl and butyl substituents, and is greater than would be expected considering the relative viscosity of this IL compared to that of the others in the series. This appears unusual if unconstrained ion diffusion is the only mode of conductivity present in these four $[C_n{}^4CNPy][NTf_2]$ ILs.

$[C_1{}^4CNPy][NTf_2]$ is the least viscous of the four ILs and shows a conductivity profile that is almost identical to that of $[C_3{}^4CNPy][NTf_2]$. The lower viscosity of $[C_1{}^4CNPy][NTf_2]$ should give rise to higher conductivity, based purely on free diffusion of the ions in the liquids and it is worth noting that $[C_1{}^4CNPy][NTf_2]$ has a rigid, planar cation that lacks a symmetry-breaking kink in the *N*-alkyl substituent.

The non-systematic changes in viscosity/conductivity for the ILs with *N*-methyl and *N*-ethyl chains compared to the two ILs with longer *N*-alkyl chains show a breakdown in the conventional conductivity-viscosity relationship, presumably through increased aggregation of the smaller ions leading to deviation from 'normal' ionic liquid behaviour. Exactly, how aggregation differs with the changes in cation, and how this may lead to the observed differences in both viscosities and conductivities across this short homologous series of the $[C_n{}^4CNPy][NTf_2]$ ILs remains open to speculation. One possible cause could be that $[NTf_2]^-$ anions are the predominant charge carriers, and that the impact of the nitrile functionalities within the cations contributes to the increased cation organisation, thus allowing pathways for anion transport.

Viscosity and Conductivity of $[C_n{}^4CNPy][NTf_2]$:1-MN CT complex liquids

On mixing each of the ILs with 1-MN at a 1:1 ratio, intensely coloured yellow-orange CT liquids are obtained, consistent with the observations previously reported. The viscosity and conductivities of the 1:1 $[C_n{}^4CNPy][NTf_2]$:1-MN mixtures were determined between *ca.* 320-410 K, except for $[C_1{}^4CNPy][NTf_2]$:1-MN where the higher melting point of the 1:1 complex necessitated a minimum temperature for measurement of 368 K. The viscosities of the four $[C_n{}^4CNPy][NTf_2]$:1-MN mixtures compared against those of the neat ILs are shown in Fig. 5 (and tabulated in ESI, Table S2).

The viscosity of $[C_4{}^4CNPy][NTf_2]$:1-MN is reduced by *ca.* 50% compared to that of the neat $[C_4{}^4CNPy][NTf_2]$ at any particular temperature. For example, from 18.9 to 10.3 mPa·s at 368 K, Fig. 5d). This decrease is broadly consistent with the anticipated impact of adding a molecular organic diluent,[30] although the reduction in viscosity measured is less than that obtained from the corresponding addition of one equivalent of acetonitrile (ESI, Table S2) where the viscosity is reduced from *ca.* 490 to 79 mPa·s

View Article Online
DOI: 10.1039/D6TA02268E

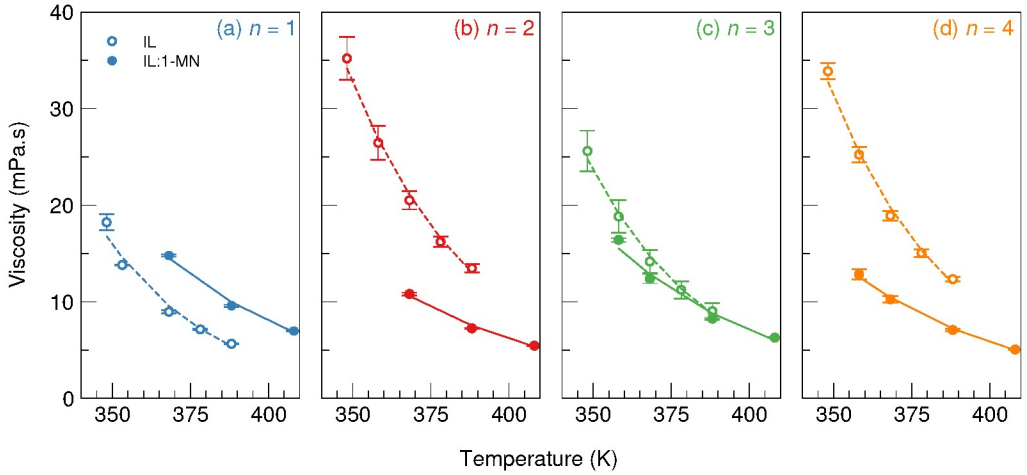

Fig. 5 Plots illustrating the different changes in viscosity upon addition of 1-MN to produce 1:1 CT complexes with (a) $[C_1{}^4CNPy][NTf_2]$, (b) $[C_2{}^4CNPy][NTf_2]$, (c) $[C_3{}^4CNPy][NTf_2]$, (d) $[C_4{}^4CNPy][NTf_2]$ showing the convergence in the viscosities of all four IL:1-MN CT complexes and the opposite effects on the viscosity between $n = 1$ with an increase in viscosity and $n = 4$ with an expected decrease in viscosity on addition of the aromatic diluent.

at 298 K.

However, only a minimal change in viscosity is observed with $[C_3{}^4CNPy][NTf_2]$ between the IL and the IL:1-NM CT-complex (Fig. 5c). For example, the viscosities of the neat IL and IL:1-MN mixtures are 14.2 and 12.4 mPa·s at 368 K, a reduction of only 12%. Compared to $[C_2{}^4CNPy][NTf_2]$, which exhibits greater than expected viscosity in the neat state, the viscosity of the $[C_2{}^4CNPy][NTf_2]$:1-MN mixture shows a much greater decrease of *ca.* 47%, similar to the reduction seen with $[C_4{}^4CNPy][NTf_2]$:1-NM, from 20.5 (neat IL) to 10.8 mPa·s (IL:1-MN) at 368 K (Fig. 5b). This large drop in viscosity may reflect disruption of the greater ion–ion aggregation present in the neat IL.

In marked contrast, the viscosity of $[C_1{}^4CNPy][NTf_2]$:1-MN is approximately 60% *greater* than that of the neat IL, $[C_1{}^4CNPy][NTf_2]$, with a rising from 8.7 (neat IL) to 14.8 mPa·s (IL:1-MN) at 368 K (Fig. 5a). All measurements were made above the melting point of the $[C_1{}^4CNPy][NTf_2]$:1-MN 1:1 complex[8] and so this increase in viscosity cannot be ascribed to the formation of a supercooled liquid state.

Surprisingly, despite the relative changes in viscosity between the neat ILs and their IL:1-MN CT complexes, which give rise to the reduced viscosity for $n = 2$ and 4, and the increase in viscosity for $n = 1$, and effectively no change when $n = 3$, the magnitudes of the viscosities of the four IL:1-MN mixtures are remarkably similar, converging to similar values (between 10-15 mPa s at 368 K) regardless of the viscosity of the original neat IL. This, and the two opposing trends in the changes in viscosity with increasing cation size (N-alkyl substituent chain length) for the neat ILs (increase) and IL:1-MN mixtures, where the increase in viscosity in the IL:1-MN mixtures for $n = 1$ is followed by a smaller sequential decrease in viscosity as associative impacts (estimated to increase viscosity for $n = 1$ by 70%) reducing to a decrease in viscosity of 12% for the IL:1-MN mixtures at $n = 2$, and a decrease of 50% for n = 4 are shown graphically in Fig. 6. By comparison, the dilution effect of MeCN gave a net drop in

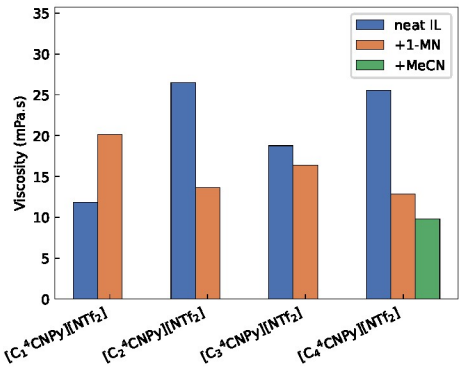

Fig. 6 Viscosities of neat ionic liquids (blue), IL:1-MN mixtures (orange) and $[C_4{}^4CNPy][NTf_2]$:MeCN (green) at 358 K (data extrapolated from the viscosity profiles in Fig. 5 for $n = 1$ and 2, and $[C_4{}^4CNPy][NTf_2]$:MeCN) showing the relative changes, with the expected increase in viscosity with cation size (as n increases) and the competing impacts of CT-association leading to an increase in viscosity compared to the neat IL ($n = 1$) through to a significant overall decrease in viscosity ($n = 4$) albeit, reduced compared to the effects of the pure diluent, MeCN.

viscosity of *ca.* 62% and we would anticipate a greater difference in relative viscosities between IL:1-MN and IL-MeCN mixtures for the smaller ILs with smaller N-alkyl groups (n = 1–3).

Notably, although all four IL:1-MN mixtures have similar viscosities, that of $[C_1{}^4CNPy][NTf_2]$:1-MN is the greatest, despite the viscosity of the neat IL being lower than that of the longer-chain members of the series. This may be associated with stronger CT complex formation between the two rigid planar aromatic components, not disrupted by the presence of a flexible *N*-alkyl substituent, or to 'anomalous' behaviour of the neat ILs compared to the CT complex-liquid mixtures (Fig. 5).

Conductivities of the CT liquids are likewise similar (Fig. 7) and increase with temperature from *ca.* 0.13–0.20 to 1.20–1.65 S m^{-1} between 320–410 K (368–410 K for the higher melting

View Article Online
DOI: 10.1039/D6TA02268E

$[C_1{}^4CNPy][NTf_2]$:1-MN system), following Arrhenius behaviour. Notably, the activation energies for conduction in the ILs are all very similar (average 31.38 kJ mol^{-1}, stdev 1.46) whereas the IL:1-MN CT mixtures show a wider range of activation energies ranging from 19.1 to 31.3 kJ mol^{-1} (average 25.85 kJ mol^{-1}, stdev 5.15) from the n = 1 to n = 4 systems, as shown in Fig. 7. A decrease in activation energy for ionic conductivity indicates facilitated charge transport, particularly at lower temperatures. The trend with decreasing *N*-alkyl chain length suggests a systematic structural contribution to transport that is less temperature-dependent than simple diffusion, consistent with reduced barriers for ion migration between sites. This behaviour may reflect a shift from constructive CT-stacking to more conventional dilution effects as n increases across the IL series. Given that bulk viscosity and conductivity are normalised for the CT-complexes with 1-MN, the observed variation in activation energy is more likely governed by the balance between CT aggregates, their dynamics and lifetimes, and their local environment. Shorter alkyl chains reduce van der Waals interactions and cation size, diminishing nanoscale segregation between polar and non-polar domains. This likely facilitates cation reorganisation and lowers the activation energy for ion transport.

A Walden plot, shown in Fig. 8, analysis provides further insight into the overall ionicity of the ILs and IL:1-MN mixtures. All the ILs, and IL:1-MN mixtures lie within the 'good IL' region (between the 10 and 100% ionicity lines),[31] indicating good ion dissociation. All systems show changes in the conductivity/viscosity products that run parallel to the ideal and 10% ionicity lines with changes in temperature indicating that there are no significant changes in the modes of ion transport and mobility with temperature. This is consistent with the independent conductivity and viscosity profiles shown in Figs 4 and 5. Similarly, the degrees of ionicity revealed in the Walden plot map to the observed conductivities, with the neat $[C_2{}^4CNPy][NTf_2]$ displaying the highest ionicity, with the remaining neat ILs and with that of all four IL:1-MN mixtures being closely clustered.

As such, this analysis does not furnish significant additional structural elucidation into the behaviour of the ionic liquids and their 1:1 mixtures with 1-MN. However, as has been reported by MacFarlane *et al.*[31] interpretation of Walden plots does not take any explicit account of the size, charge, or modes of charge transport within systems and, from Harris[32] that a Walden plot can only, at best, give a qualitative ranking of behaviour in concentrated ionic media and "*cannot and should not be used for classifying the interactions in ionic liquids*".

The convergence and common magnitudes of both viscosity and conductivity across this series of ILs upon CT complexation suggests that a common conduction modes dominated by anion mobility is induced within the similarly organised liquid matrices. This is likely to be a result of π-cation stacking that reorganises the liquid structure, disrupting ion-ion association where it is strong (*e.g.* in $[C_2{}^4CNPy][NTf_2]$) and, in the case of $[C_1{}^4CNPy][NTf_2]$, introducing supramolecular organisation that increases resistance to flow.

Insights from vibrational spectroscopy

$[NTf_2]^-$ anions conformer distribution and environment. The low frequency range of the Raman spectrum provides information about anion conformations, in particular the relative intensities of peaks between 250–430 cm^{-1} reflects the population of *cis* and *trans* isomers of the $[NTf_2]^-$ anion.[33] In $[C_1{}^4CNPy][NTf_2]$ and $[C_2{}^4CNPy][NTf_2]$, the anion is primarily in the *trans* form, while a mixture of *cis* and *trans* is deducible for $[C_3{}^4CNPy][NTf_2]$ and $[C_4{}^4CNPy][NTf_2]$ (Figure 9).

Specifically, the prevalence of the lower energy *trans* isomer can be deduced from the absence of the mode at 326 cm^{-1}, which is characteristic of the *cis* form only.[33] In $[C_2{}^4CNPy][NTf_2]$, the signature bands of the *trans* conformer $[NTf_2]^-$ anion, at 315 and 342 cm^{-1}, are of extremely high intensity under excitation with the 785 nm laser compared to those of the other ILs, which is not the case when using the 532 nm laser. We hypothesise that this may be due to a wavelength-dependent enhancement effect in the near IR. The observation of bands due to solely *trans* anions in $[C_1{}^4CNPy][NTf_2]$ and $[C_2{}^4CNPy][NTf_2]$, and a combination of *cis* and *trans* conformers for $[C_3{}^4CNPy][NTf_2]$ and $[C_4{}^4CNPy][NTf_2]$ is consistent with the physical forms of the respective ILs at RT. $[C_1{}^4CNPy][NTf_2]$ and $[C_2{}^4CNPy][NTf_2]$ are solids that have previously been shown crystallographically to have *trans* conformer $[NTf_2]^-$ anions,[6] whereas the RT liquid $[C_3{}^4CNPy][NTf_2]$ and $[C_4{}^4CNPy][NTf_2]$ salts contain a dynamic distribution of both $[NTf_2]^-$ anion conformers.[7]

In the interaction sensitive region of the Raman spectra (720–760 cm^{-1}), the strong band at around 741 cm^{-1}, assigned to the S-N-S stretch mode of the $[NTf_2]^-$ anion,[34] undergoes a small red-shift from $[C_1{}^4CNPy][NTf_2]$ to $[C_4{}^4CNPy][NTf_2]$ (Figure 10a).

The higher frequency of this stretching mode for $[C_1{}^4CNPy][NTf_2]$, compared to $[C_3{}^4CNPy][NTf_2]$ and $[C_4{}^4CNPy][NTf_2]$, is consistent with the differences in environment, solid rather than liquid. However, the red-shifted position for $[C_2{}^4CNPy][NTf_2]$ (see also Table 1) is remarkable considering this IL is in the solid state. This red-shift is typically assigned to a reduction in association and interaction of the $[NTf_2]^-$ anions. Hence, in $[C_2{}^4CNPy][NTf_2]$, the anions are 'more free' than in $[C_1{}^4CNPy][NTf_2]$, despite both ILs being in the solid state. It should be mentioned that DFT calculations predict a lower frequency for the *cis* isomer compared to the *trans*. More specifically, the peculiarity is that the Raman signal for $[C_2{}^4CNPy][NTf_2]$ is shifted to lower frequency than that of the liquid $[C_3{}^4CNPy][NTf_2]$ and $[C_4{}^4CNPy][NTf_2]$, which have fluxional anions with both *cis* and *trans* populations. It appears that in $[C_2{}^4CNPy][NTf_2]$, the $[NTf_2]^-$ anion adopts the *trans* isomer most typically observed in the solid state or organic $[NTf_2]^-$ salts, as evidenced from the anion conformational signals shown in Fig. 9, but that cation–anion association is weaker than that found in $[C_1{}^4CNPy][NTf_2]$, with the anion experiencing a net coordination environment that is as weakly associated as that of the liquid analogues. This may reflect an intrinsically poorer packing of cations and anions in the solid state for $[C_2{}^4CNPy][NTf_2]$ that gives rise to rotational disorder

View Article Online
DOI: 10.1039/D6TA02268E

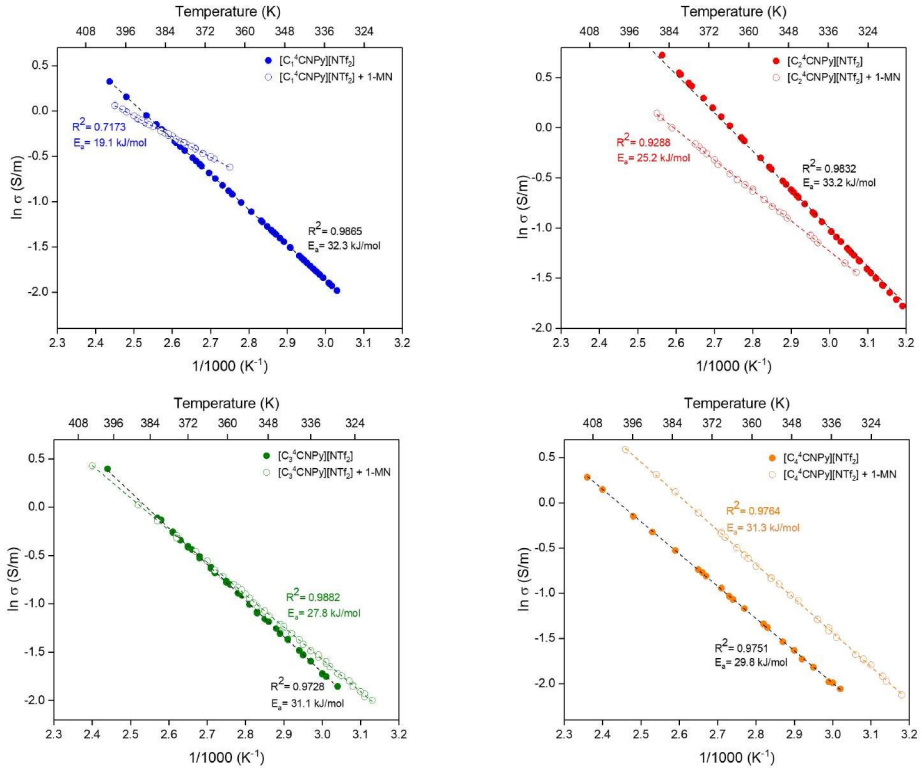

Fig. 7 Comparison of the conductivities of neat [C$_n$^{4}CNPy][NTf$_2$] ILs and their IL:1-MN CT-complexes (n = 1–4; neat IL, open symbols; CT-complex, closed symbols) as a function of temperature showing Arrhenius behavior over this temperature range and a gradual reduction in the activation energy for conduction as the alkyl-chain on the cation is shortened from butyl to methyl.

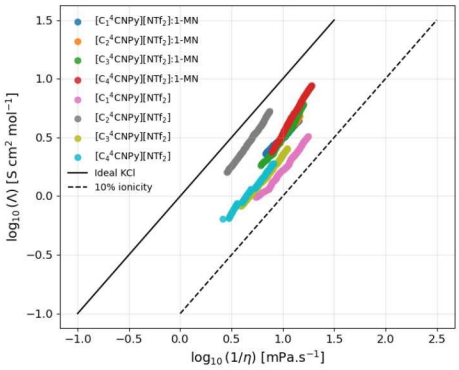

Fig. 8 Walden plot comparing the viscosity and conductivity of the four ILs and their IL:1-MN mixtures.

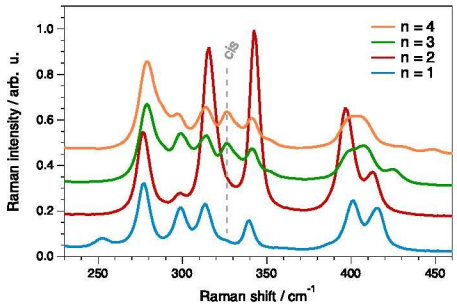

Fig. 9 The anion conformation region of the Raman spectra (250–450 cm^{-1}) for neat [C$_n$^{4}CNPy][NTf$_2$] ILs under 785 nm laser excitation showing the characteristic signatures for *trans* [NTf$_2$]$^-$ anions in solid [C$_1$^{4}CNPy][NTf$_2$] and [C$_2$^{4}CNPy][NTf$_2$] and a bands deriving from both *cis* and *trans* conformers in the liquids, [C$_3$^{4}CNPy][NTf$_2$] and [C$_4$^{4}CNPy][NTf$_2$].

about the SO$_2$–N–SO$_2$ region of the anions, as originally reported for the crystal structure of [C$_2$^{4}CNPy][NTf$_2$].[6]

In the spectral range 1050–1300 cm^{-1}, which includes vibrational modes from the –SO$_2$– and –CF$_3$ groups of the [NTf$_2$]$^-$ anion (Fig. 11), the position of the –CF$_3$ mode does not change from [C$_1$^{4}CNPy][NTf$_2$] to [C$_2$^{4}CNPy][NTf$_2$], whereas the –SO$_2$– mode is blue shifted from 1134 cm^{-1} in [C$_1$^{4}CNPy][NTf$_2$] to 1138 cm^{-1} in [C$_2$^{4}CNPy][NTf$_2$], possibly reflecting shorter S=O bonds due to weaker interactions that could also be associated with S–N–S disorder in the anion in the solid state as previously observed in the crystal structure of [C$_2$^{4}CNPy][NTf$_2$].[6]

Cation–cation interactions. Differences in the net cation–anion association modes in [C$_2$^{4}CNPy][NTf$_2$] compared to the other ILs is also supported by the relative shifts in the cation nitrile stretching around 2200–2300 cm^{-1} (Fig. 10b). The nitrile stretch in [C$_2$^{4}CNPy][NTf$_2$] has a higher wavenumber compared to those for [C$_3$^{4}CNPy][NTf$_2$] and [C$_4$^{4}CNPy][NTf$_2$], which is rationalisable due to the changes in state between the ethyl and propyl/butyl-functionalised ILs. However, the –C≡N stretch in [C$_2$^{4}CNPy][NTf$_2$] is also blue-shifted by 2.5 cm^{-1} with

View Article Online
DOI: 10.1039/D6TA02268E

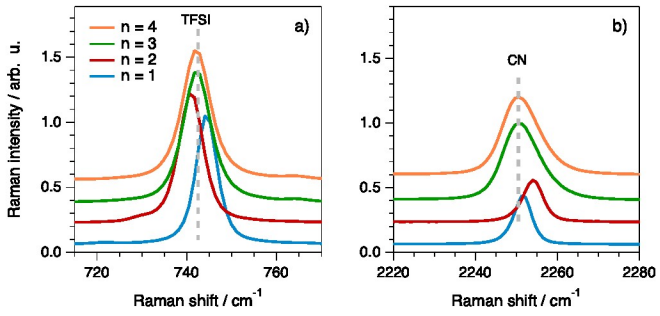

Fig. 10 Raman stretching signals from $[NTf_2]^-$ anion asymmetric stretch at *ca.* 740 cm^{-1} (left) and the $[C_n{}^4CNPy]^+$ cation nitrile stretch at 2250 cm^{-1} (right).

Table 1 Peak positions for the $[NTf_2]^-$ anion S−N−S and cation C≡N stretch bands in the ILs $[C_n{}^4CNPy][NTf_2]$ (n = 1–4). Peak position and shapes were fitted with a Voigt function from the spectra shown in Fig. 10

n	Anion S−N−S stretch /cm^{-1}	FWHM	Cation C≡N stretch /cm^{-1}	FWHM
1	744.4	3.5	2251.5	3.2
2	740.9	4.1	2254.0	3.6
3	742.3	4.1	2251.1	7.6
4	742.1	4.0	2251.0	8.2

respect to $[C_1{}^4CNPy][NTf_2]$. The higher wavenumber indicates a stronger, shorter C≡N bond and this implies weaker interactions with its chemical surroundings. This is supported from the lengths of the respective C(2)-H···N-C hydrogen bonds formed between cations in the crystal structures reported in reference 6.

In the high frequency range, spectra collected with excitation using the 532 nm laser reveal the C−H stretching modes of the cation alkyl group below 3050 cm^{-1} and aromatic ring C−H stretches in the peak at 3107 cm^{-1}. This latter band appears significantly broader for $[C_2{}^4CNPy][NTf_2]$ than for $[C_1{}^4CNPy][NTf_2]$ (Figure 12), suggesting greater structural disorder for $[C_2{}^4CNPy][NTf_2]$.

Impact of CT complex formation with 1-MN. Finally, upon addition of 1-MN to the neat ILs, some subtle spectral changes can be observed, as shown in Figure 13 for two key vibrational modes. In all samples, the −C≡N stretching mode around 2250 cm^{-1} red-shifts in the IL:1-MN mixture, although this is most remarkable with $[C_2{}^4CNPy][NTf_2]$. The $[C_2{}^4CNPy][NTf_2]$:1-MN mixture also exhibits a blue-shift of the anion mode at *ca.* 741 cm^{-1} relative to the neat IL. For $[C_1{}^4CNPy][NTf_2]$:1-MN, the vertical dashed lines in Figure 13 mark the position of the vibrational modes as recorded using the 532 nm laser which, despite a large luminescent background, contained distinct resolvable peaks.

Mechanistic considerations

We attribute the anomalous behaviour of $[C_2{}^4CNPy][NTf_2]$ in the neat state to cation-cation association, which elevates viscosity while leaving sufficient pathways for $[NTf_2]^-$ mobility, yielding higher-than-expected conductivity decoupled from the higher

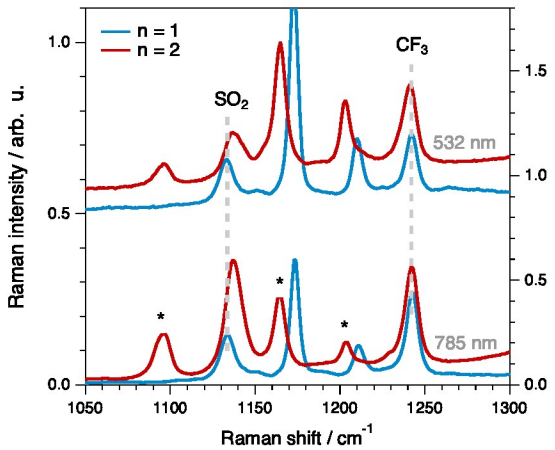

Fig. 11 Raman spectra in the spectral range 1050–1300 cm^{-1} where vibrational modes involving the $-SO_2-$ and $-CF_3$ groups appear, recorded with excitation using the 532 nm (top traces) and the 785 nm (bottom traces) lasers for $[C_1{}^4CNPy][NTf_2]$ (blue) and $[C_2{}^4CNPy][NTf_2]$ (red).

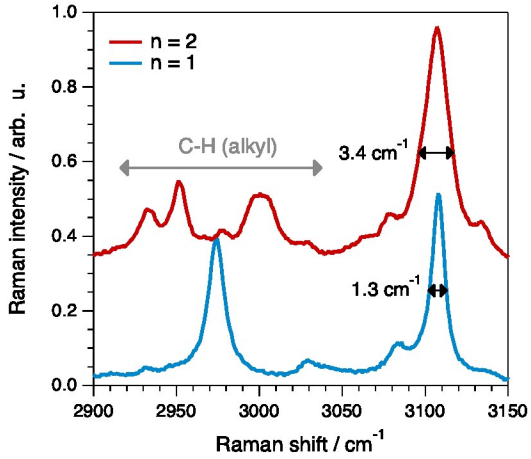

Fig. 12 Raman spectra in the region of alkyl and ring C−H stretching modes, for the samples $[C_1{}^4CNPy][NTf_2]$ (blue) and $[C_2{}^4CNPy][NTf_2]$ (red).

viscosity.[35] We propose that the enhanced viscosity of neat $[C_2{}^4CNPy][NTf_2]$ compared to the analogues with n = 3 and 4 could be associated with cation-pairing through the polar electron-withdrawing nitrile group. This potential cation-pairing or aggregation might then lead to larger and therefore more slowly moving cationic domains in the liquid and generate pathways for freer, less associated anions to move, thereby giving rise to a greater conductivity through anion mobility within the liquid that is more viscous than might be expected based on purely ion-size or volume considerations.

The room temperature Raman spectra of $[C_2{}^4CNPy][NTf_2]$ (Fig. 11 and 10) reveal that, at least in the solid state, the ion-associations observable in the previously reported crystal structure[7] can be observed spectroscopically. The red-shift in the $[NTf_2]^-$ anion asymmetric stretch, associated with reduced cation–anion association could be a result of sub-optimal crystal packing, supported by conformational-disorder of the anion

View Article Online
DOI: 10.1039/D6TA02268E

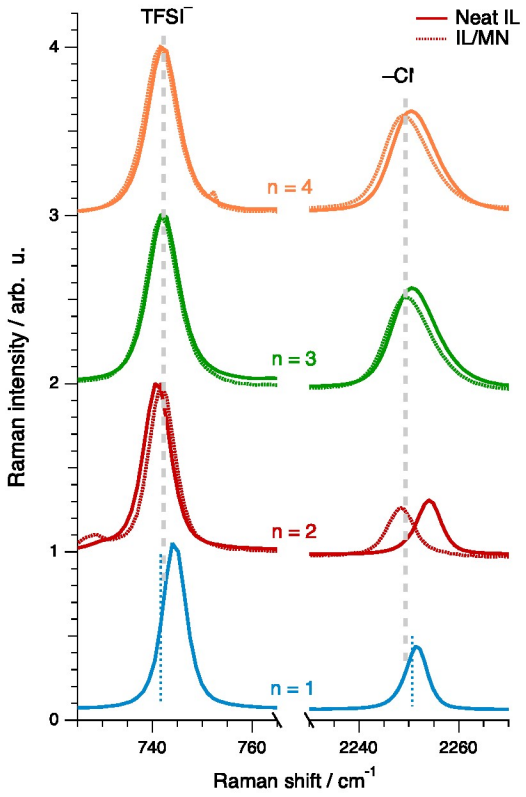

Fig. 13 Raman spectra in the spectral ranges of the [NTf2] characteristic mode (725–765 cm^{-1}) and the C–N stretching mode (2230–2270 cm^{-1}), for all ILs (solid lines) and IL:1-MN mixtures (dashed lines). Vertical, large-dashed lines are simply guides to the eye.

S-N-S central group in the crystal, that arises from enhanced cation-cation association. Again, this association is evident in the cation nitrile stretch in Fig. 10, and if this is conserved through melting to the liquid state, then both increased viscosity (larger cationic aggregates) and increased conductivity (less constrained anions) can be rationalised, or at least postulated.

In contrast, the IL:1-MN mixtures all display similar viscosities which, for $[C_2{}^4CNPy][NTf_2]$ and $[C_4{}^4CNPy][NTf_2]$ are reduced from those of neat ILs, and is largely invariant for $[C_3{}^4CNPy][NTf_2]$, but has an increase for $[C_1{}^4CNPy][NTf_2]$. The conductivity profiles also normalise to similar values (*ca.* 1 S m^{-1} at 400 K). CT complexation realigns the series by substituting cation-cation contacts with cation-aromatic stacking, reducing viscosity and normalising transport mechanisms irrespective of the size of the *N*-alkyl group.

For $[C_4{}^4CNPy][NTf_2]$, with the longer *N*-alkyl chain of the ILs examined, addition of 1-MN results in a reduction in viscosity and commensurate increase in conductivity. This could be simply ascribed to addition of an organic diluent, although the magnitude of viscosity reduction is lower than that observed with the addition of acetonitrile. However for $[C_1{}^4CNPy][NTf_2]$, with an N-methyl group, addition of 1-MN induces an opposite effect, increasing viscosity and decreasing conductivity. This points to the constructive role of CT-complex association between *N*-alkyl-cyanopyridinium cations and 1-MN as a liquid modifier that is in competition with the impact of the diluent effect which appears to be more pronounced for the ILs with longer N-alkyl substituents on the cation. This is presumably because an organic diluent primarily interacts with the van der Waals regions of the liquids, rather than with the charge–charge Coulombic structure that dominates in ionic liquids.

With $[C_3{}^4CNPy][NTf_2]$, both the viscosity and conductivity are unchanged between the neat IL and IL:1-MN mixture which is consistent with a balance and neutralisation of the associative effects of CT-complex structuring and organic diluent dissociation of the liquid. Remarkably, despite the higher than expected viscosity and conductivity of $[C_2{}^4CNPy][NTf_2]$ that do not follow the series trends, the IL:1-MN mixture does not have correspondingly anomalous behaviour and is both less viscous and less conductive than the neat IL, with values that converge with those from the other three ILs in the series. Formation of cation-aromatic CT-complex motifs in $[C_2{}^4CNPy][NTf_2]$:1-MN is disruptive to proposed cation-cation association in the neat IL that gives rise to higher than anticipated viscosity and realigns the behaviour of the IL:aromatic mixture with the remainder of the series.

This is supported by the self-diffusion data obtained from a combination of ^1H and ^{19}F DOSY NMR spectroscopy. Diffusion coefficients for each proton in the cations, and for each proton in 1-MN, were similar and the mean value, averaged across all proton signals from the respective cation and 1-MN components of the samples, and from the single ^{19}F signal of the anion, are shown in Fig. 14 and Table 2.

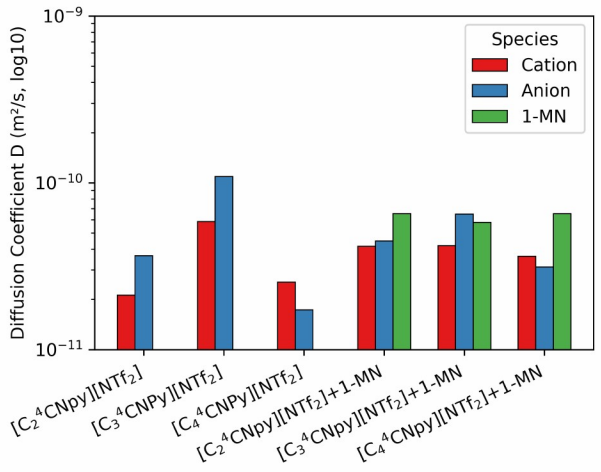

Fig. 14 Diffusion coefficients of the $[C_n{}^4CNPy]^+$ (n = 2–4) cations, $[NTf_2]^-$ anions and 1-MN at 60 °C determined from ^1H and ^{19}F DOSY NMR spectroscopy on the neat ILs and IL:1-MN mixtures.

As can be seen from Fig. 14, the diffusion coefficients obtained for the neat ILs are largely consistent with magnitudes anticipated by comparison with other ILs containing $[NTf_2]^-$ anions[16,19,27,36] and mirror the relative changes in bulk viscosity measured for the neat ILs and IL:1-MN mixtures. That is, both D_{cation} and D_{anion} of the relatively low viscosity $[C_3{}^4CNPy][NTf_2]$ are larger than those of the more viscous $[C_2{}^4CNPy][NTf_2]$ and $[C_4{}^4CNPy][NTf_2]$ analogues. Notably, and again consistent with bulk viscosity, the self-diffusion coefficients in the IL:1-MN

View Article Online
DOI: 10.1039/D6TA02268E

Table 2 Diffusion coefficients (D_+ for cations and D_- for anions, $\times10^{-11}$ m^2 s^{-1}) of the $[C_n{}^4CNPy]^+$ (n = 2–4) cations, $[NTf_2]^-$ anions and 1-MN at 60 °C determined from ^{1}H and ^{19}F DOSY NMR spectroscopy on the neat ILs and IL:1-MN mixtures. In contrast, in 1:1 $[C_4{}^4CNPy][NTf_2]$:MeCN, D_+ = 7.91 $\times10^{-11}$ m^2 s^{-1} and D_{MeCN} = is 4.20$\times10^{-10}$ m^2 s^{-1}.

	Neat IL		IL:1-MN CT complex		
	D_+	D_-	D_+	D_-	D_{1-MN}
$[C_2{}^4CNPy][NTf_2]$	2.12	3.66	4.17	4.48	6.52
$[C_3{}^4CNPy][NTf_2]$	5.86	10.9	4.20	6.49	5.79
$[C_4{}^4CNPy][NTf_2]$	2.54	1.73	3.63	3.13	6.53

mixtures all converge to similar values (*ca.* 5×10^{-11} m^{2}s^{-1}) for all ions and 1-MN, with the magnitudes of D_{cation} and D_{1-MN} much more closely correlated supporting association when compared to those for the non-CT-forming mixture of $[C_4{}^4CNPy][NTf_2]$ with MeCN. For the $[C_4{}^4CNPy][NTf_2]$:MeCN system, the diffusivity of the $[C_4{}^4CNPy]^+$ cation D_{cation} increases from 2.54$\times10^{-11}$ m^2 s^{-1} in the neat IL to 7.91$\times10^{-11}$ m^2 s^{-1} consistent with the reduction in bulk viscosity of the mixture and double that of the cation in the IL:1-MN mixture (D_{cation} = 3.63$\times10^{-11}$ m^2 s^{-1}) with D_{MeCN} of 4.20$\times10^{-10}$ m^2 s^{-1}. This much greater self-diffusivity of MeCN is consistent with the size of the molecular diluent and decoupling from the motion of the $[C_4{}^4CNPy]^+$ cation in the absence of CT-complex formation.

Conclusions

The motivation behind this study was to examine whether CT-aggregation and stacking in these IL:aromatic mixtures, originally identifies with $[C_1{}^4CNPy][NTf_2]$:1-MN by Hardacre *et al.*[8] were of sufficient length and persistence to give rise to electronic conduction pathways. Our results can neither prove, or disprove this hypothesis at present, since electronic conduction is likely to occur at a rate significantly faster than the maximum frequency we were able to scan to during the impedance measurements. Moreover, due to the comparatively small resistance that would be associated with electronic compared to ionic conduction, it is also likely that features associated with this may not be visible in the real impedance spectra.[37]

Notwithstanding the lack of direct evidence for bulk electronic conduction, these studies have explored the conductivities and viscosities of neat $[C_n{}^4CNPy][NTf_2]$ ILs and their liquid CT complexes with 1-MN, and demonstrates how charge-transfer complexation can profoundly alter the transport properties of these nitrile-functionalised pyridinium ionic liquids. Neat $[C_n{}^4CNPy][NTf_2]$ salts exhibit both viscosity and conductivity characteristics that deviate from simple homologous trends. $[C_2{}^4CNPy][NTf_2]$ shows unexpectedly high viscosity yet relatively high conductivity, suggesting enhanced cation-cation association and dominant anion mobility. Addition of 1-methylnaphthalene, as an exemplar polyaromatic π-rich electron donor, produces highly coloured CT complex liquids at 1:1 IL:aromatic in which both viscosity and conductivity profiles are normalised across the series, indicating disruption of the ion-ion aggregation present in the neat ILs and formation of organised cation-aromatic stacks. The effect of CT complex formation in the IL:1-MN liquids as a structure-making associative interaction is most evident for $[C_1{}^4CNPy][NTf_2]$ where the cation is rigid and planar and manifests as an increase in viscosity and a reduction in the bulk conductivity. In contrast, with $[C_4{}^4CNPy][NTf_2]$, the impact of CT aggregation is off-set by the effect of dilution, presumably through interactions between 1-MN and the N-butyl chains of the IL cation. These two opposing effects are in balance for $[C_3{}^4CNPy][NTf_2]$ where the addition of one molar equivalent of 1-MN has almost no impact on either the viscosity or conductivity on moving from neat IL to the IL:1-MN mixture.

The systematic change in the activation energy for conduction in the IL:1-MN mixtures, decreasing as the N-alkyl chain becomes shorter, is consistent with modified nanoscale structure and potential anion-mobility pathways along organised domains. The convergence of the transport properties in the CT-complex liquids highlights the potential of π-cation interactions as a design tool for tuning ionic liquid behaviour, with implications for advanced electrolytes and functional soft materials.

Acknowledgement

The authors also gratefully acknowledge the UK EPSRC for providing a PhD studentship to AEK (grant number EPSRC/S3809ASA) as well as the Chalmers Area of Advance Materials Science for supporting an Amanuensis position, and the Competence Centre Tech4H2. Tech4H2 is hosted by Chalmers University of Technology and is financially supported by the Swedish Energy Agency (P2021-90268) and the member companies Volvo, Scania, Siemens Energy, GKN Aerospace, PowerCell, Oxeon, RISE, Stena Rederier AB, Johnsson Matthey and Insplorion.

Conflicts of interest

There are no conflicts to declare

Data Availability

The data supporting this article have been included as part of the Supplementary Information.

References

1 D. R. MacFarlane, M. Forsyth, P. C. Howlett, M. Kar, S. Passerini, J. M. Pringle, H. Ohno, M. Watanabe, F. Yan, W. Zheng, S. Zhang and J. Zhang, *Nature Reviews Materials*, 2016, **1**, 15005.

2 I. Y. López-Cortés, G. A. Iglesias-Silva, M. Ramos-Estrada and J. L. Rivera-Rojas, *Fluid Phase Equilibr.*, 2020, **514**, 112543.

3 (*a*) A. Boruń, *J. Mol. Liq.*, 2019, **276**, 214–224; (*b*) O. Nordness and J. F. Brennecke, *Chem. Rev.*, 2020, **120**, 12873–12902.

4 (*a*) A. Stoppa, J. Hunger and R. Buchner, *J. Chem. Eng. Data*, 2008, **54**, 472–479; (*b*) E. T. Fox, E. Paillard, O. Borodin and W. A. Henderson, *J. Phys. Chem. C*, 2012, **117**, 78–84.

5 (*a*) J. N. Canongia Lopes, M. F. Costa Gomes, P. Husson, A. A. H. Pádua, L. P. N. Rebelo, S. Sarraute and M. Tariq, *J. Phys. Chem. B*, 2011, **115**, 6088–6099; (*b*) J. E. Bara, A. Finotello, J. W. Magee, S. Qian, K. E. O'Harra, G. P. Dennis and R. D. Noble, *J. Chem. Eng. Data*, 2019, **58**, 17956–17964; (*c*) J. E. Bara, A. Finotello, J. W. Magee and R. D. Noble, *J. Ionic Liq.*, 2023, **3**, 100050.

6 C. Hardacre, J. D. Holbrey, C. L. Mullan, M. Nieuwenhuyzen, W. M. Reichert, K. R. Seddon and S. J. Teat, *New J. Chem.*, 2008, **32**, 1953–1967.

7 C. Hardacre, J. D. Holbrey, C. L. Mullan, M. Nieuwenhuyzen, T. G. A. Youngs and D. T. Bowron, *J. Phys. Chem. B*, 2008, **112**, 8049–8056.

8 C. Hardacre, J. D. Holbrey, C. L. Mullan, M. Nieuwenhuyzen, T. G. A. Youngs, D. T. Bowron and S. J. Teat, *Phys. Chem. Chem. Phys.*, 2010, **12**, 1842–1853.

9 (*a*) J. D. Holbrey and C. L. Mullan, *Ionic liquids and their use in extraction processes*, European Patent Application EP1854786A1, 2007, `https://data.epo.org/publication-server/rest/v1.0/publication-dates/20071114/patents/EP1854786NWA1/document.html`, Applicant: BP p.l.c., Publication date: 14 November 2007, Filing date: 4 September 2006;

View Article Online
DOI: 10.1039/D6TA02268E

(*b*) J. D. Holbrey, I. López-Martin, G. Rothenberg, K. R. Seddon, G. Silvero and X. Zheng, *Green Chem.*, 2008, **10**, 87–92.

10 S. H. McCalmont, G. Simon, H. Q. N. Gunaratne, M. Costa Gomes, D. M. Wilkins, J. D. Holbrey and L. Moura, *ACS Sustainable Chem. Eng.*, 2025, **13**, 11770–11783.

11 H. Tahara, Y. Tanaka, S. Yamamoto, S. Yonemori, B. Chan, H. Murakami and T. Sagara, *Chem. Sci.*, 2021, **12**, 4872–4882.

12 D. Rochefort, *Curr. Opin. Electrochem.*, 2019, **15**, 125–132.

13 (*a*) R. J. Bushby, S. D. Evans, O. R. Lozman, A. McNeill and B. Movaghar, *J. Mater. Chem.*, 2001, **11**, 1982–1984; (*b*) S. Sergeyev, W. Pisula and Y. H. Geerts, *Chem. Soc. Rev.*, 2007, **36**, 1902–1929; (*c*) T. Wöhrle, I. Wurzbach, J. Kirres, A. Kostidou, N. Kapernaum, J. Litterscheidt, J. C. Haenle, P. Staffeld, A. Baro, F. Giesselmann and S. Laschat, *Chem. Rev.*, 2015, **116**, 1139–1241.

14 U. Domańska, K. Walczak and M. Zawadzki, *J. Chem. Thermodyn.*, 2014, **69**, 27–35.

15 P. Bonhôte, A.-P. Dias, M. Armand, N. Papageorgiou, K. Kalyanasundaram and M. Grätzel, *Inorg. Chem.*, 1996, **35**, 1168–1178.

16 H. Tokuda, K. Hayamizu, K. Ishii, M. A. B. H. Susan and M. Watanabe, *J. Phys. Chem. B*, 2004, **108**, 16593–16600.

17 (*a*) K. R. Seddon, A. Stark and M.-J. Torres, *Pure Appl. Chem.*, 2000, **72**, 2275–2287; (*b*) J. A. Widegren, A. Laesecke and J. W. Magee, *Chem. Commun.*, 2005, 1610–1612.

18 J. M. Crosthwaite, M. J. Muldoon, J. K. Dixon, J. L. Anderson and J. F. Brennecke, *J. Chem. Thermodyn.*, 2005, **37**, 559–568.

19 H. Tokuda, K. Ishii, M. A. B. H. Susan, S. Tsuzuki, K. Hayamizu and M. Watanabe, *J. Phys. Chem. B*, 2006, **110**, 2833–2839.

20 A. Nazet, S. Sokolov, T. Sonnleitner, S. Friesen and R. Buchner, *J. Chem. Eng. Data*, 2017, **62**, 2549–2561.

21 L. Qing-Shan, Y. Pei-Fang, Y. Miao, T. Zhi-Cheng, L. Chang-Ping and W.-B. Urs, *Acta Phys. Chim. Sin.*, 2011, **27**, 2762–2766.

22 (*a*) H. Tokuda, S. Tsuzuki, M. A. B. H. Susan, K. Hayamizu and M. Watanabe, *J. Phys. Chem. B*, 2006, **110**, 19593–19600; (*b*) Q.-G. Zhang, S.-S. Sun, S. Pitula, Q.-S. Liu, U. Welz-Biermann and J.-J. Zhang, *J. Chem. Eng. Data*, 2011, **56**, 4659–4664; (*c*) M. Dzida, M. Musiał, E. Zorębski, M. Zorębski, J. Jacquemin, P. Goodrich, Z. Wojnarowska and M. Paluch, *J. Mol. Liq.*, 2019, **278**, 401–412; (*d*) C. Reinado, A. Pelegrina, M. Sánchez-Rubio, H. Artigas and C. Lafuente, *J. Chem. Eng. Data*, 2022, **67**, 636–643.

23 A. Kazakov, J. Magee, R. Chirico, V. Diky, K. Kroenlein, C. Muzny and M. Frenkel, *Ionic Liquids Database - ILThermo (v2.0)*, 2013.

24 D. Wu, A. Chen and C. Johnson, *J. Magn. Reson, A*, 1995, **115**, 260–264.

25 E. O. Stejskal and J. E. Tanner, *J. Chem. Phys.*, 1965, **42**, 288–292.

26 M. G. Del Pópolo, C. L. Mullan, J. D. Holbrey, C. Hardacre and P. Ballone, *J. Am. Chem. Soc.*, 2008, **130**, 7032–7041.

27 H. Tokuda, K. Hayamizu, K. Ishii, M. A. B. H. Susan and M. Watanabe, *J. Phys. Chem. B*, 2005, **109**, 6103–6110.

28 (*a*) H. A. Every, A. G. Bishop, D. R. MacFarlane, G. Orädd and M. Forsyth, *Phys. Chem. Chem. Phys.*, 2004, **6**, 1758–1765; (*b*) C. Schreiner, S. Zugmann, R. Hartl and H. J. Gores, *J. Chem. Eng. Data*, 2009, **55**, 1784–1788; (*c*) T. Makino, M. Kanakubo, Y. Masuda, T. Umecky and A. Suzuki, *Fluid Phase Equilibr.*, 2014, **362**, 300–306; (*d*) M. S. Calado, J. C. F. Diogo, J. L. Correia da Mata, F. J. P. Caetano, Z. P. Visak and J. M. N. A. Fareleira, *Int. J. Thermophys.*, 2013, **34**, 1265–1279.

29 E. Dahlqvist, E. M. Morais and A. Martinelli, *J. Mol. Liq.*, 2024, **415**, 126269.

30 D. Warmińska and I. Cichowska-Kopczyńska, *J. Mol. Liq.*, 2020, **304**, 112754.

31 D. R. MacFarlane, M. Forsyth, E. I. Izgorodina, A. P. Abbott, G. Annat and K. Fraser, *Phys. Chem. Chem. Phys.*, 2009, **11**, 4962.

32 K. R. Harris, *J. Phys. Chem. B*, 2019, **123**, 7014–7023.

33 (*a*) A. M. Moschovi, S. Ntais, V. Dracopoulos and V. Nikolakis, *Vib. Spectrosc.*, 2012, **63**, 350–359; (*b*) V. H. Paschoal, L. F. O. Faria and M. C. C. Ribeiro, *Chem. Rev.*, 2017, **117**, 7053–7112; (*c*) L. F. O. Faria, T. A. Lima and M. C. C. Ribeiro, *Crystal Growth Design*, 2017, **17**, 5384–5392.

34 J. Nishida, J. P. Breen, B. Wu and M. D. Fayer, *ACS Cent. Sci.*, 2018, **4**, 1065–1073.

35 M. Salanne, C. Simon, P. Turq and P. A. Madden, *J. Phys. Chem. B*, 2007, **111**, 4678–4684.

36 A. Noda, K. Hayamizu and M. Watanabe, *J. Phys. Chem. B*, 2001, **105**, 4603–4610.

37 A. E. Bumberger, A. Nenning and J. Fleig, *Phys. Chem. Chem. Phys.*, 2024, **26**, 15068–15089.

Modulating transport properties in N-alkyl-4-cyanopyridinium ionic liquids through formation of liquid charge transfer complexes

View Article Online
DOI: 10.1039/D6TA02268E

Aloisia E. King,[a] Josh Bailey,[a] Jiabo Le,[a] Adam H Turner,[a,b] Rudra N. Purusottam,[a] Eva Dahlqvist,[c] Anna Martinelli,[c] Małgorzata Swadźba-Kwaśny[a] and John D. Holbrey[a*]

[a] *The QUILL Research Centre, School of Chemistry and Chemical Engineering, Queen's University Belfast, David Keir Building, Stranmillis Road, Belfast BT9 5AG, UK. E-mail: j.holbrey@qub.ac.uk*

[b] *Current address: Department of Chemistry, Ateneo de Manila University, Quezon City 1108, Philippines*

[c] *Department of Chemistry and Chemical Engineering, Chalmers University of Technology, Gothenburg 41296, Sweden*

Data availability statement

The data supporting this article have been included as part of the Supplementary Information.